Author/s:
Sarwar, T;Ramamohanarao, K;Zalesky, A

Title:
A critical review of connectome validation studies

Date:
2021-12-01

Citation:
Sarwar, T., Ramamohanarao, K. & Zalesky, A. (2021). A critical review of connectome validation studies. NMR in Biomedicine, 34 (12), https://doi.org/10.1002/nbm.4605.

Persistent Link:
https://hdl.handle.net/11343/298983

Sarwar T. (Orcid ID: 0000-0001-7313-5350)

Title

A Critical Review of Connectome Validation Studies

Authors

T. Sarwar*[1], K. Ramamohanarao[2], A. Zalesky*[3,4]

Affiliations

[1] School of Computing Technologies, RMIT University, Victoria, 3000, Australia

[2] Department of Computing and Information Systems, The University of Melbourne, Victoria 3010, Australia

[3] Melbourne Neuropsychiatry Centre, The University of Melbourne, Victoria, 3010, Australia

[4] Department of Biomedical Engineering, The University of Melbourne, Victoria, 3010, Australia

***Corresponding author:**
Tabinda Sarwar
School of Computing Technologies
RMIT University
Victoria, 3000, AUSTRALIA
Phone: +61451063616
Email: tabinda.sarwar@rmit.edu.au

Figures: 4
Tables: 2
Word count: 7950

This is the author manuscript accepted for publication and has undergone full peer review but has not been through the copyediting, typesetting, pagination and proofreading process, which may lead to differences between this version and the Version of Record. Please cite this article as doi: 10.1002/nbm.4605

List of Abbreviations:

Terminology	Explanation
CoCoMac	Collations of Connectivity data on the Macaque brain
COMMIT	Convex Optimization Modeling for Microstructure Informed Tractography
CSD	Constrained Spherical Deconvolution
DSI	Diffusion Spectrum Imaging
DTI	Diffusion Tensor Imaging
HARDI	High Angular Resolution Diffusion Imaging
LiFE	Linear Fascicle Evaluation
SIFT	Spherical-deconvolution Informed Filtering of Tractograms

Abstract:

Diffusion MRI tractography is the most widely used macroscale method for mapping connectomes *in vivo*. However, tractography is prone to various errors and biases, and thus tractography-derived connectomes require careful validation. Here, we critically review studies that have developed or utilized phantoms and tracer maps to validate tractography-derived connectomes, either quantitatively or qualitatively. We identify key factors impacting connectome reconstruction accuracy, including streamline seeding, propagation and filtering methods, and consider the strengths and limitations of state-of-the-art connectome phantoms and associated validation studies. These studies demonstrate the inherent limitations of current fiber orientation models and tractography algorithms and their impact on connectome reconstruction accuracy. Reconstructing connectomes with both high sensitivity and specificity is challenging, given that some tractography methods can generate an abundance of spurious connections, while others can overlook genuine fiber bundles. We argue that streamline filtering can minimize spurious connections and potentially improve the biological plausibility of connectomes derived from tractography. We find that algorithmic choices such as the tractography seeding methodology, angular threshold and streamline propagation method can substantially impact connectome reconstruction accuracy. Hence, careful application of tractography is necessary to reconstruct accurate connectomes. Improvements in diffusion MRI acquisition techniques will not necessarily overcome current tractography limitations without accompanying modeling and algorithmic advances.

1. Introduction:

Diffusion-weighted magnetic resonance imaging (dMRI) can be used to non-invasively infer microstructural properties of the brain. Tractography is a reconstruction method based on dMRI to compute the trajectories of white matter (WM) fiber bundles. The primary objective of tractography is to reconstruct non-invasively WM fiber bundles from dMRI. More recently, tractography has been used to map the human structural connectome [1-3] *i.e.* a comprehensive network description of WM fiber bundles connecting pairs of gray matter (GM) regions (also referred to as structural connectivity). Structural connectomes model the physical links between brain regions, whereas functional connectomes represent the network of functionally connected regions. These connectomes are a static representation of the brain that could change over time [4, 5]. When referring to connectomes in this review, we specifically mean structural connectomes mapped with tractography.

Generally, connectome mapping using tractography is a five-step process involving: (1) dMRI acquisition (2) segmenting the cortex into Regions of Interest (ROIs - cortical parcellation) (3) diffusion/fiber orientation estimation (4) streamline generation using tractography, and (5) linking pairs of ROIs with streamlines to build a connectivity matrix. Fiber orientation models [6-19] and tractography [20-38] involve an indirect estimation of microstructural properties, making them prone to errors and biases [39]. Many of the

orientation estimation models impose different constraints on the dMRI acquisition, such as the number of diffusion-weighting gradients, their strength (b-value), and Signal-to-Noise (SNR) ratio, along with the assumptions associated with signal models. Moreover, tractography itself depends on numerous constraints, which include angular threshold, seeding methodology, number of streamlines, and termination criteria. With all of these algorithmic choices, the impact of tractography methods on connectome mapping is not well-understood, particularly given the absence of a "gold standard" enabling assessment of reconstructed connectomes.

Hence, given that tractography is an indirect method of reconstructing WM fiber bundles, it is important to measure its accuracy and precision. Phantoms with a known ground truth have been used extensively for evaluating tractography. These can be divided into three broad categories: i) Physical phantoms comprising synthetic or natural fibers that mimic the geometry of neuronal fiber tracts; ii) tracer maps derived from invasive axonal tract-tracing; iii) numerical phantoms generated by simulating fiber trajectories according to a given model. While tracer studies are considered a more accurate (albeit invasive) technique for mapping WM fiber bundles than tractography, tracers are not errorless mapping techniques and thus they are sometimes referred to as a "silver standard" [40]. Guidance on the design of phantoms for tractography validation can be found in [41-44]. Many such phantoms exist in the literature [45-52], which have been successfully used to evaluate the performance of fiber estimation models and tractography algorithms. The objective of these studies is to evaluate the accuracy of the local fiber orientation estimation and the geometrical properties (curvature and spatial extent) of the estimated fiber bundles. The impact of various tractography-specific parameters like angular threshold [53, 54], step-size [53, 55, 56] and seeding methodology [57, 58]) and dMRI-specific parameters (diffusion-weighted gradients [48, 59], b-value [47-49, 59, 60] and Signal-to-Noise Ratio- SNR [49, 61]) have been evaluated using phantoms. The association between microstructural properties and their functional implications has been extensively studied in the presence and absence of neurological disorders to analyze the WM bundles [62-64].

Tractography validation studies suggest that current tractography outcomes are biased to a certain extent. Complex fiber architectures involving crossing fibers are challenging to resolve and current models of diffusion can either overlook certain fiber populations or infer spurious populations. Estimation of spurious orientations at the local scale can result in the reconstruction of spurious fiber bundles. Common Gaussian reconstruction models cannot fully represent fiber bundle characteristics, including intra- and extra-axonal compartment, axonal density, and tissue complexity [65]. Hence, a local diffusion model that fails to detect certain fiber orientations can result in tractography failing to detect the corresponding fiber bundles. Moreover, accurate modeling of local fiber orientations does not necessarily imply accurate tractography reconstruction [66].

Connectomes are typically mapped based on the locations of streamline endpoints. If the endpoints of sufficiently many streamlines reside within two separate regions, those regions

are considered structurally connected, irrespective of the geometrical properties of the streamlines [67]. Thus, streamline geometry is therefore not explicitly modeled when mapping connectomes.

In contrast to conventional criteria used to evaluate tractography (*e.g.* tract geometry, spatial extent, *etc.*), evaluating tractography in the context of connectome mapping is primarily concerned with the presence/absence of fiber bundles between pairs of regions and connection strengths. The geometric properties of a reconstructed fiber bundle are less of a consideration in connectomics. Given the inherent challenges and limitations of tractography and fiber estimation [39, 47, 68], it is important to evaluate the extent to which these limitations impact the connectome mapping process [67]. Network analyses of connectomes provide valuable insight into brain disorders [69-71], cognition [72, 73], and developmental changes [74, 75], and thus understanding the limitations of current connectome mapping algorithms is crucial to ensure the validity of these insights.

Here, we review studies that developed or utilized phantoms and tracer maps to validate connectomes mapped with tractography either qualitatively or quantitatively. While many phantoms have been developed for validating brain microstructure inferred from dMRI [44, 76-80], we will restrict our review to studies that have evaluated connectomes mapped with tractography. Section 2 describes the background and nomenclatures used in this review. Section 3, 4 and 5 discusses studies that have used physical phantoms, tracer maps, and numerical phantoms for evaluating tractography reconstructed connectomes, respectively. These sections discuss the findings and conclusions reported from the validation studies, which can help to identify the key factors that affect the accuracy of the reconstructed connectome. After reviewing the outcomes of the connectome validation studies, we briefly review recent methodological advances aimed to improve the accuracy and biological plausibility of tractography-derived connectomes in Section 6, including streamline filtering, thresholding and related advanced algorithms.

2. Background:

We begin by providing a brief overview of key terminology and a summary of the nomenclatures used for describing these algorithms and technical concepts. A brief overview of tractography and fiber orientation models is presented in the appendix (Table A1).

Fiber tract/bundle: a group of tightly packed axons following a common spatial trajectory in WM. Tractography aims to estimate the trajectories of these fiber bundles/tracts non-invasively.

Streamline: a computer-generated curvilinear map approximating the trajectory of an underlying fiber bundle.

Structural connection: a monosynaptic axonal connection between a pair of regions enabled by a fiber bundle. Distinct from functional connectivity, which refers to statistical dependencies in brain activity.

Connectome: a comprehensive network description of structural connectivity.

Connection density: proportion of non-zero connections to the total number of connections that could be formed in a brain network (connectome).

Connectivity strength: a measure of the strength of connectivity associated with a structural connection. With tractography, it is often measured as the number of interconnecting streamlines between a pair of regions (streamline count). It is important to note that streamline counts are not necessarily proportional to the number of axons in a fiber tract.

Nomenclatures:

Table 1: List of nomenclatures

Terminology	Explanation	Terminology	Explanation
CoCoMac	Collations of Connectivity data on the Macaque brain	COMMIT	Convex Optimization Modeling for Microstructure Informed Tractography
COMMIT2	Variant of COMMIT	CSD	Constrained Spherical Deconvolution
dMRI	Diffusion-weighted magnetic resonance imaging	DSI	Diffusion Spectrum Imaging
DTI	Diffusion Tensor Imaging	EEW	Errors of the Edge Weights
FA	Fractional Anisotropy	FPR	False-Positive Rate
FOD	Fiber-Orientation Distribution function	GM	Gray Matter
HARDI	High Angular Resolution Diffusion Imaging	IB	Invalid Bundle
IC	Invalid Connection	LiFE	Linear Fascicle Evaluation
NC	No Connection	PVE	Partial Volume Effect
ROI	Region-of-Interest	SIFT	Spherical-deconvolution Informed Filtering of Tractograms
SIFT2	Variant of SIFT	SNR	Signal-to-Noise Ratio

TPR	True-Positive Rate	VB	Valid Bundle
VC	Valid Connection	WM	White Matter

3. Physical Phantoms

Physical phantoms for evaluating tractography are composed of materials that can represent the anisotropic diffusion in WM fiber bundles. Generally, this can be achieved by using synthetic, natural, or glass materials for constructing the fiber trajectories. Von dem Hagen and Henkelman [45] were the first to develop a physical phantom to study the effect of fiber orientations on diffusion profile in terms of the apparent diffusion coefficient. The phantom comprised water-filled polytetrafluoroethylene fibers, with an inner diameter of 50 μm and an outer diameter of 325 μm. The fibers were arranged to study the effect of changing and multiple fiber orientations, by winding the plastic fibers in parallel, coiled and random orientations. Many other physical phantoms were later developed to evaluate the validity of estimated microstructures and fiber bundles. The material of the fibers used for these phantoms included glass capillaries [81], acrylic fibers [48] , rayon fibers [82], polyester [83], hemp and linen [84], plastic [47], dyneema [85], cotton [52], and *ex-vivo* rat spinal cords [86]. These fibers were either doped or immersed in a liquid (*e.g.* pure water, aqueous solutions) to generate the microstructural properties, which can be measured using the diffusion-weighted signal [44].

The beforementioned phantoms were primarily used to evaluate the accuracy of either the local diffusion/fiber orientation estimation models or tractography algorithms for reconstructing the synthetic fibers. "FiberCup" is another physical phantom that was used to quantitatively evaluate 10 tractography algorithms [87]. The phantom was manufactured using acrylic fibers of diameter 20 μm, enclosed in a polyurethane case. The phantom was filled with distilled water under vacuum conditions and the remaining air bubbles were destroyed with an ultrasound beam. Seven fiber bundles were modeled targeting bending, crossing, kissing, and fanning configurations found in the coronal section of the human brain (Figure 1). The study primarily focused on evaluating the spatial accuracy of estimated fiber bundles. The "FiberCup" phantom was later simulated under varying fractional anisotropy (FA) and b-values using "Fiberfox", an open-source framework for simulating WM fiber tracts, to compare the connectomes reconstructed by state-of-the-art algorithms (deterministic, probabilistic, and global) [88]. The validity of the connectome was quantified in terms of sensitivity, specificity and sum of errors of the edge weights (EEW).

The Fiberfox study reported that for lower FA values (<0.13), tractography performance using the simple tensor model was similar to the sophisticated models (Constrained Spherical Deconvolution-CSD, Persistent Angular Structure, Q-ball). This was the case for both the physical and simulated "FiberCup". As the physical "FiberCup" phantoms had low FA (average ≈0.1), the same phantom was simulated for evaluating the tractography under high FA values. For high FA, probabilistic tractography algorithms showed a higher deviation

from the ground truth in comparison to deterministic algorithms and hence were not recommended for mapping connectomes. Overall, deterministic CSD had the best performance in terms of EEW. The effect of various artifacts (Rician noise, distortion, Gibbs ringing, thermal noise, ghosting) on the estimated connectome was also investigated using the simulated "FiberCup". The results demonstrated that Rician, ghosting, and thermal noise resulted in a substantial increase in the error and the number of false connections, whereas image distortion and Gibbs ringing artifact had a minor impact on the connectivity analysis. It should be noted that except for the Fiberfox study, physical phantoms have not been used to evaluate measures of structural connectivity.

Although physical phantoms offer control on generating fiber bundles, this method is limited to relatively simple fiber architectures comprising a few fiber bundles, given that manufacturing these phantoms is often challenging. A physical connectome phantom will further require specification of the physical regions within a phantom to represent GM, which could be challenging. To solve this issue, these regions can be virtually assigned at the endpoints of the fiber bundles. To date, physical phantoms to evaluate structural connectivity in the context of connectomics have not been developed.

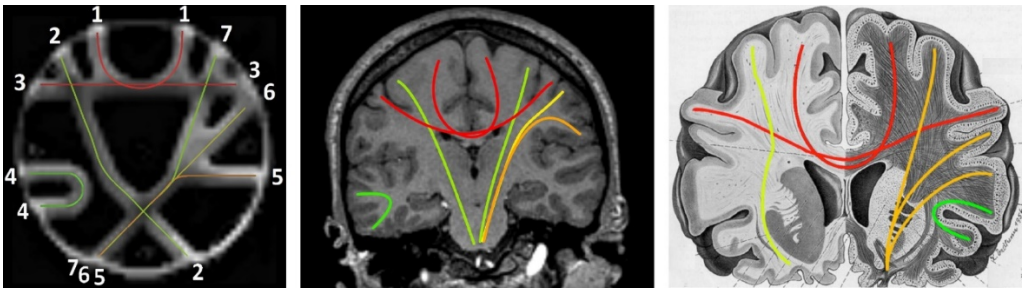

Figure 1. FiberCup imitating a coronal slice of the brain with short 'U' fibers (bundle 4), left-to-right hemisphere commissural projections (bundle 3), larger 'U' and fanning bundles representing corpus callosum (bundle 1) and corticospinal tract (bundles 2, 5, 6 and 7) respectively. Reproduced from [57]

4. Tracer Maps

Tracer studies enable the mapping of axonal trajectories using invasive chemical tracers. While tracer studies are invasive, the extracted WM maps are generally considered accurate as they represent the microstructural properties of real brain tissues. In comparison to physical and numerical phantoms, tracer maps are extensively used to evaluate microstructure estimation models [89, 90] or the spatial properties of WM estimated by tractography [37, 51, 91]. The estimated WM bundles have been validated using various performance metrics *e.g.,* FA, mean diffusivity, root-mean-square error, *etc.* for both normal (healthy) and pathological subjects [40, 92-94]. This validation method has been extended to estimate tracer-based connectivity matrices for evaluating connectomes.

Histological dissection is another well-known invasive validation method that provides ground truth for qualitatively evaluating fiber bundles derived from tractography. Dissection (Klingler's method [95, 96]) and myelin staining have been successfully used to validate the accuracy of estimated fiber bundles [97, 98]. Given that dissection is laborious and time-consuming, this method is generally limited to qualitative evaluation of a few selected fiber bundles, *e.g.* a recent study used dissection to validate the reconstruction of vertical occipital fasciculus and its projections to the visual cortex [99].

Impact of local orientation estimation and tractography algorithm

Numerous diffusion fiber orientation estimation models and tractography models can be found in the literature (Table A1). The variation in tractography estimation is generally observed for different local orientation models. For example, due to the inability of the tensor model to resolve multi-fiber configurations, tractography-derived streamlines may be inaccurate for geometrically complex fiber bundles [82]. Similarly, the inter-variability in the reconstructed connectomes by different categories of the tractography algorithms is also expected for the same local orientation estimation model. A squirrel monkey connectome mapped using tensor-based deterministic and probabilistic tractography reported that probabilistic tractography did not provide a higher correlation with the ground truth in comparison to deterministic methods [100]. A macaque connectome estimated by deterministic Generalized Q-ball Imaging tractography showed a correlation of 0.25–0.31 with the tracer estimated connectivity matrix [101]. On the other hand, a higher correlation of 0.59 was reported between connectomes reconstructed by probabilistic tractography, where the fiber orientations were estimated by an improved ball and stick method [102]. For a mouse brain, a correlation of 0.46 between the probabilistic tractography estimated and tracer-based connectivity matrix was reported [103]. Hence, variability in the reconstructed connectome is observed for different orientation estimation models and tractography algorithms where the choice of the algorithm depends on the application. Readers are referred to [66, 104] for further details on the validation of local orientation models and tractography algorithms.

Impact of user-defined tractography parameters

Tractography depends on various user-defined parameters, which include step-size, angle threshold, stopping criteria (FA/Fiber Orientation Distribution-FOD threshold), and seeding methodology. Variation in these parameters can generate different tractograms that can potentially estimate different connectomes. Aydogan and colleagues [105] evaluated compartment-based FOD probabilistic tractography estimated connectomes under varying tractography parameters against tracer maps. This study demonstrated that the overlap between tractography and tracer injection experiments changes dramatically with different choices of parameter combinations. Lower FOD threshold ($< 2.25 \times 10^{-2}$) and step-size (50μm)

increased the true positive rate (TPR) and false positive rate (FPR), whereas lower values of angle threshold and the number of streamlines had an adverse effect on connectome reconstruction. This phenomenon was also supported by Thomas and colleagues [54] *i.e.* optimal results can only be achieved by optimizing tractography parameters. Sinke and colleagues [106] also reported the variability in TPR and FPR under varying conditions (connection density, streamline, angle and FA/FOD threshold). So far, optimal values of these user-defined parameters do not exist.

Sensitivity and specificity

Tractography evaluation studies have reported the estimation of false fiber bundles, which were not a part of the underlying "ground-truth" phantom [57]. Hence, it is expected that tractography estimates false connections along with the true connections but for high accuracy, the number of the false connections should be minimal. Many validation studies have confirmed generation of FPs. Calabrese and colleagues [103] conducted the first study to map the mouse connectome using probabilistic tractography, which was compared against a neuronal tracer map. They reported a TPR of 61% and FPR of 26% for probabilistic tractography. In another study, Diffusion Spectrum Imaging (DSI)-based tractography was used to map the connectome of the fascicularis monkey, which was quantitively compared against ground truth from the CoCoMac (Collations of Connectivity data on the Macaque brain [107]) database [108]. CoCoMac comprises more than four hundred published tracing macaque studies. The study concluded that the accuracy of the connectome is a trade-off between TPR and FPR *e.g.* for a specificity of 90%, the sensitivity dropped to 40%. A common consensus among these studies is the presence of FPs for estimated connectomes, even for the optimal connectome reconstructed using optimal tractography parameters [54] (Figure 2). A tractography algorithm that demonstrates high sensitivity is much likely to have low specificity [109]. Post-mortem human connectome study by Seehaus and colleagues [110] is an exception that showed high sensitivity and specificity of ≈80%. As the validation setting varied for these studies, a direct comparison between them is not possible.

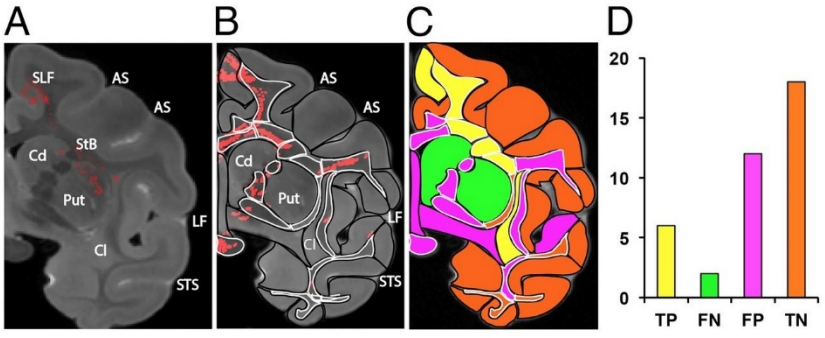

Figure 2: Assessing the anatomical accuracy of tractography algorithms (A) The red dots indicate the topography of axonal pathways following the injection of an anterograde tracer in the left precentral gyrus (PCG) (B) For each dMRI slice that was anatomically matched with the histology slice from the reference atlas, the GM (black lines) and WM (white lines) regions were manually segmented and parcellated into discrete ROIs. The red dots represent the location of axonal pathways as determined with the Q-ball tractography (C) The agreement between tracer and tractography results was computed for each slice. The colors indicate ROIs that were categorized as true positives (TP), true negatives (TN), false positives (FP), and false negatives (FN). (D) Histogram showing the TP, TN, FP, and FN for the specific slice where FPs are higher than TPs. AS, arcuate sulcus; Cd, caudate; Cl, claustrum; LF, lateral fissure; Put, putamen; SLF, superior longitudinal fasciculus; StB, striatal bundle; STS, superior temporal sulcus. (Reprinted from [54])

Reconstruction of true connections

Although FPs are inevitable, validation studies have confirmed that tractography can estimate a high percentage of TPs. For the macaque visual system, Azadbakht and colleagues [111, 112] reported an average connectome mapping accuracy of 74% and demonstrated a good correspondence between the tracer map and tractography-derived connectivity under a connection strength threshold of 10%. Zakszewski and colleagues [113, 114] demonstrated that the connectivity maps obtained from probabilistic tensor tractography were largely consistent with the macaque tracer maps. Gao and colleagues [100] also found approximately 75–98% of streamlines reached the correct ROIs. These studies confirm that regardless of the limitation, challenges, and biases in the indirect WM estimation process, tractography can estimate true connections providing valuable information about the *in vivo* brain.

Impact of microstructural properties

In addition to the fiber/diffusion orientation models and tractography algorithms, the estimation of connections also depends on the microstructural properties of the tissues. This phenomenon is evident for complex fiber configurations which is a bottleneck for many tractography algorithms. Knösche and colleagues [40] reported that tractography was able to estimate the true fiber tracts, but FP connections were also generated due to the presence of complex WM configuration. It is well-known that Diffusion Tensor Imaging (DTI) is unable to adequately model complex WM microstructure because it assumes a Gaussian diffusion profile. In comparison, Diffusion Kurtosis Imaging, HARDI (High Angular Resolution Diffusion Imaging) and other multi-fiber models have successfully resolved some of the limitations of DTI [57, 115, 116]. While these models have addressed the resolution of multi-fiber complex configuration with good local performance, the current tractography algorithm cannot achieve good global performance for connectome reconstruction [66]. The qualitative evaluation of macaque's connectome demonstrated that the complex arrangement of superficial fibers impeded tractography by acting as barriers between the cortex and deep WM, irrespective of HARDI modeling and high-quality data [98]. The study reported that ≈50% of cortical locations were affected by these superficial fibers, limiting the detectability of cortical connections. GM–WM partial volume effect (PVE) can further pose difficulties in identifying the terminating fiber bundles [51].

Gyral bias refers to the difficulty in tracing highly-curved axonal trajectories across WM-GM boundaries in gyral blades, which can affect the performance of tractography algorithms [117]. Schilling and colleagues [118] investigated the impact of gyral bias by comparing tractography against myelin histology performed on a Rhesus macaque brain. This effect was evident for single and multi-fiber implementations (tensor and CSD) of deterministic or probabilistic tractography, though the bias introduced in tensor-based tractography was larger than CSD-based tractography. Connectomic studies [98, 119] have also reported the estimation of inaccurate cortical connections in the presence of gyral bias.

The distance between the regions also results in the estimation of FPs and false negatives (FNs), especially for regions separated at a longer distance [111, 112]. Sinke and colleagues [106] demonstrated that the number of FPs and FNs increased with the fiber length where probabilistic CSD outperformed global tractography for the reconstruction of long-range connections. An exponential relationship between connection weight and fiber length was found for macaque's connectome [102]. Readers are referred to [120, 121] for further details on the challenges the underlying anatomical and microstructural properties pose on the connectome mapping process.

Impact of parcellation resolution

The coarseness of GM parcellation is a relatively arbitrary choice that influences the process of connectome mapping [122]. The reliability of the tensor-based deterministic tractography in constructing connectomes for three cortical parcellations of 69, 96 and 300 nodes was studied for a mouse brain [123]. For the optimal selection of tractography parameters for each parcellation, the accuracy of reconstructed connectomes with 69 and 96 regions was higher than the connectome with 300 regions. But the tractography performed equally well for 69 and 96 regions. Thus, the study concluded that an appropriate scale of parcellation scheme was critical in constructing a reliable connectome along with the optimal tractography parameter selection. The dependency of connectome accuracy on the resolution of parcellation was also observed for tracer study in squirrel money, where the accuracy reduced for high-resolution GM subdivisions [100].

Most connectome validation studies focus on parcellated connectomes, where connectivity is estimated between brain regions delineated using a parcellation atlas. Alternatively, high-resolution connectomes can be mapped at the resolution of individual voxels/vertices, thereby avoiding the need for a parcellation atlas [124]. The analysis of high-resolution connectomes (voxel/vertices-wise connectivity matrix) can provide advantages relative to parcellated connectomes, including improved spatial localization of effects [125]. But currently, generating and analyzing high-resolution connectomes is computationally expensive [126].

Connectivity strength and network analysis of connectomes

As previously mentioned, the connectome evaluation is primarily concerned with the absence/presence of connections and their connectivity strength. Graph theory has served as an important tool for evaluating the network properties of the reconstructed connectomes [127, 128]. Ideally, the network properties and strengths of the connections should be preserved in the reconstructed connectome. But as tractography is not perfect, some deviation in these characteristics is expected. Shen and colleagues [129] found an agreement between tracer and tractography for the strength of the connected fiber bundles for macaque brain. A similarity in topological properties like degree and modularity was also observed, but a mismatch was identified for hubs. In another macaque study [130], the strengths of the extracted corticocortical interconnections were comparable to the tracer map but variability in terms of small-world properties, hub identification, and hemispheric asymmetry was reported under varying seeding methodologies [131]. The study proposed that usage of thresholded tract volume instead of streamlines count as the index for connectivity strength could reduce the distance-bias effect for probabilistic tractography. On the other hand, Donahue and colleagues demonstrated that the tractography became less correlated with tracer as strong connections were removed progressively [102]. Generally, the tracer maps and tractography estimated connections is challenging due to the mismatch in the two modalities, which is why the majority of the validation studies have analyzed binary connectomes.

5. Numerical Phantoms

In comparison to tracer studies, numerical phantoms offer a degree of controllability and definability of fiber tracts for generating a ground truth. Hence, they provide flexibility for simulating dMRI with complex geometries under a wide range of acquisition conditions (*e.g.* b-values, SNR and diffusion-weighted gradients). The majority of numerical phantom validation studies have evaluated tractography under varying conditions (acquisition and user-defined tractography control parameters [47-49, 59-61]). But it should be noted that the findings of the numerical connectome validation studies support the conclusions drawn from tracer maps. The prominent conclusions on which these studies agree include variation in connectome's accuracy under varying tractography parameters and the inevitability of FPs.

For evaluating the state-of-the-art tractography algorithms, Côté and colleagues [57] proposed an online evaluation and validation system, namely Tractometer. The study utilized the simulated "FiberCup" phantom to compare tractography algorithms under varying user-defined control parameters which included seeding methodologies, angle thresholds and step-sizes. Specifically, deterministic and probabilistic HARDI tractography algorithms were evaluated in terms of fiber bundle coverage and connectivity metrics. Five new metrics were

proposed for evaluating the reconstructed connectome, namely; valid connections (VCs), invalid connections (ICs), no connections (NCs), valid bundles (VBs) and invalid bundles (IBs). Variation in the results was observed for the beforementioned control parameters. The study concluded that more seeds per voxel resulted in a higher number of IC and the variation in results was also observed for both ROI-based and whole-brain seeding methodology. The study recommended that careful seeding is necessary to control valid/invalid connections, as the number of IBs was lower when single seed and ROI-based seeding was used. Moreover, aggressive stopping criteria for tractography algorithms led to a large number of NCs, emphasizing the need to incorporate anatomical information to improve the tractography. The study also reported that probabilistic algorithms produced a higher number of IC and NC, whereas deterministic algorithms exhibited the best VC/IC trade-off in the connectivity analysis at the expense of lower average bundle coverage (the ratio of voxels traversed by the streamlines to the total number of voxels in the bundle). Probabilistic algorithms were found to maximize this ratio.

In contrast to the simplified "FiberCup" phantom comprising only 7 fibers, Maier-Hein and colleagues [132] simulated human brain dMRI of 25 major long-range bundles that covered 71% of the WM. The ground truth tracts were obtained by performing whole-brain global tractography on a high-quality *in vivo* dMRI followed by manual extraction. An open international tractography challenge (ISMRM 2015 Tractography Challenge) was conducted in which 96 distinct submissions were evaluated against the generated phantom. The connectivity metrics proposed in Tractometer study [133] were used for quantitative evaluation. The study reported that the majority of the state-of-the-art algorithms reproduced 90% of the ground truth bundles along with a high number of IBs. The study demonstrated that high-quality data improved the spatial properties of the fiber bundles (bundle volumetric overlap and overreach) but this improvement was not reflected in the overall accuracy of the reconstructed connectome results *i.e.* a reduction in the FP bundles was not observed. This implies that high-quality data may improve the performance of tractography, but it is not the primary factor and novel developments are needed to address the inherent limitation of diffusion models and tractography. The study emphasized that the goal of the next-generation tractography algorithms is to reconstruct the spatial extent of existing fiber bundles while controlling the FP connections.

To evaluate the connectome mapping accuracy of contemporary algorithms, Sarwar and colleagues [134] simulated numerical phantoms with predefined connectivity matrices, where tubular fibers connected pairs of ROIs defined on the surface of the sphere. The endpoints of the streamlines residing within a pair of ROIs were used to map the connectivity matrices under varying streamline thresholds. The study concluded that the tensor-based tractography was limited in mapping accurate connectomes due to the inability to resolve multi-fiber configurations (Figure 3). On the other hand, CSD-based probabilistic algorithm produced a large number of spurious connections. CSD-based deterministic tractography yielded the best performance in terms of the F-measure. The study demonstrated that it is

essential to omit connections with the fewest number of streamlines (thresholding) when using probabilistic algorithms for mapping connectomes. The study suggests that multi-fiber deterministic tractography is well suited for connectome mapping, regardless of the streamline threshold.

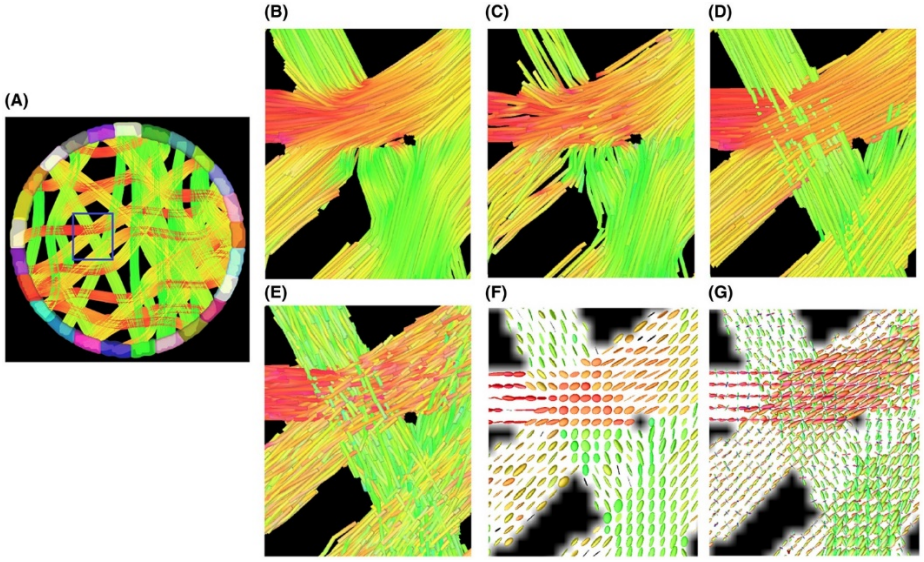

Figure 3. Ground-truth streamline trajectories (A) Streamlines in the region encapsulated by the blue rectangular box are shown for (B) Tensor based deterministic tractography (C) Tensor based probabilistic tractography (D) CSD based deterministic tractography (E) CSD based probabilistic tractography (F) local Tensor (G) local FODs (Reprinted from [134])

6. Advanced Methods to Improve Connectome Validity

Although tractography has inherent limitations and challenges, it remains the only non-invasive method to map structural connectivity using *in vivo* data [66]. The quantitative evaluation of connectomes (sections 2-4) has reported that current tractography algorithms can achieve high sensitivity at the compromise of low specificity. Hence, reducing the number of FP connections is a major challenge in connectomics. Azadbakht and colleagues [111, 112] also proposed that tractography should be corrected to account for distance bias, given that uncorrected tracking leads to a high percentage of FPs, especially at a short distance. Similarly, based on the outcomes of the 3-D Validation of Tractography with Experimental MRI (3D-VoTEM) challenge at the International Symposium on Biomedical Imaging (ISBI) 2018 in which 176 distinct tractograms were submitted, Schilling and colleagues [135] suggested that tractography alone is incapable of achieving high accuracy and incorporating additional information (*e.g.* priors based on known neuroanatomy, microstructural information) will potentially improve performance.

Filtering methods

A number of studies have proposed filtering methods to improve the accuracy and biological plausibility of tractography-derived measures of structural connectivity. For example, spherical-deconvolution informed filtering of tractograms (SIFT-[136]) recursively selects a subset of the reconstructed streamlines that closely corresponds with the underlying WM diffusion signal. Specifically, the proposed filtering is guided by FODs of the diffusion signal computed by spherical deconvolution. The FOD lobes are used to estimate the density of the fiber population, which is matched against the cross-sectional area of the streamlines to remove any streamline that does not align with the underlying diffusion model, thereby increasing the biological relevance of filtered streamlines [137]. A computationally efficient variant of SIFT, referred to as SIFT2 [138], was proposed that does not involve recursively removing streamlines from the reconstructed tractogram. Instead, SIFT2 assigns an appropriate "weight" to the streamlines which is the representation of an effective cross-sectional area for each streamline. Thus, SIFT2 retains the entire reconstructed tractogram in contrast to SIFT.

Pestilli and colleagues [139] also optimized the tractography-generated connectome by estimating a weight for each streamline, where streamlines with positive weight are retained. The diffusion signal is predicted for each streamline estimated by tractography. The proposed linear fascicle evaluation (LiFE) method utilizes the difference between the predicted and measured diffusion to quantify the prediction error. LiFE solves a set of simultaneous linear equations to assess the connectome in predicting the diffusion data, yielding a weight for each streamline demonstrating its contribution in predicting the diffusion signal. Daducci and colleagues [140] proposed a similar methodology, namely, Convex Optimization Modeling for Microstructure Informed Tractography (COMMIT). COMMIT uses a global convex optimization algorithm to fit the measured diffusion signal, where the diffusion signal generated by the streamlines is predicted as a combination of multiple compartments (intra-, extra- axonal and isotropic).

Recently, Schiavi and colleagues [141] proposed an improved version of COMMIT, referred to as COMMIT2. This method not only considers the microstructural properties of the tissues but also the prior knowledge of brain anatomy, where anatomical priors are extracted by partitioning the streamlines into bundles followed by bundle regularization. The study reported that in comparison to the aforementioned methodologies, COMMIT2 is a robust approach for improving the specificity of the connectome. Figure 4 demonstrates that these advanced filtering methods can effectively remove FPs from the reconstructed connectome, thereby improving the accuracy. It should be noted that COMMIT2 filtering involves a decision at the level of fiber bundles, while other methods filter the individual streamlines.

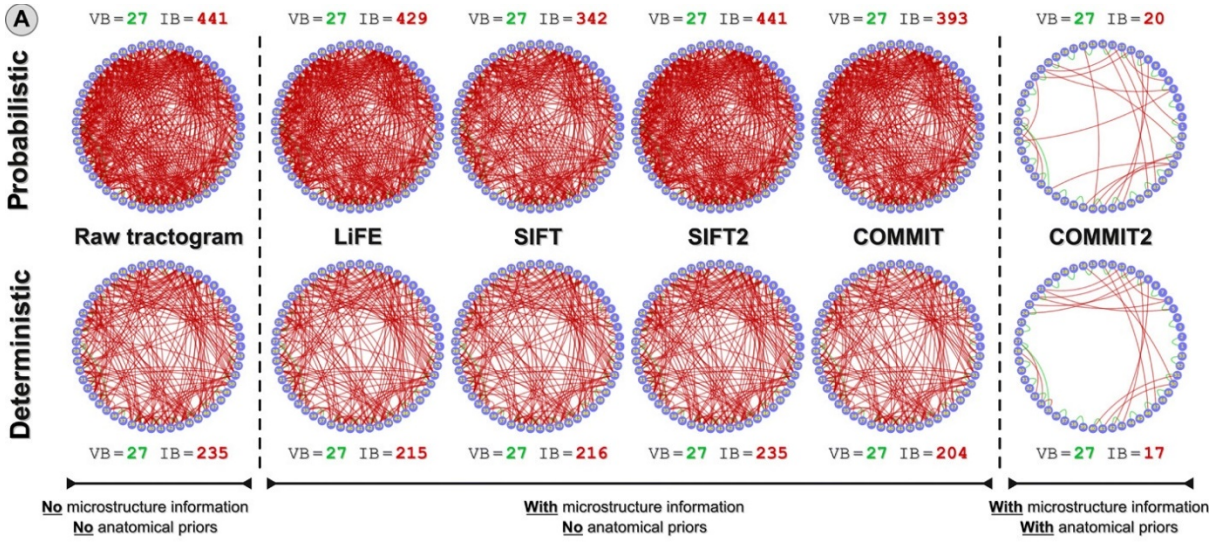

Figure 4: Sensitivity and specificity of the tractography generated connectomes before and after applying filtering methods: LiFE, SIFT, SIFT2 COMMIT and COMMIT2. Valid bundles (VBs) and invalid bundles (IBs) are reported in green, and red respectively. Reproduced from [141]

The aforementioned methods primarily considered processing the streamlines estimated by tractography without considering the geometrical properties of the extracted bundles. Zhang and colleagues [142] proposed a population-based structural connectome mapping framework that addressed the geometrical properties (shape, size and location) of the fiber bundles for removing inconsistent streamlines to improve the accuracy of the estimated connectome. The framework consists of dilating the cortical regions to generate a tractogram followed by a streamline cutting method. This procedure ensures that the extracted parts of streamlines connect a pair of regions, as streamlines can pass through multiple regions especially for the subcortical regions. Later, streamlines that did not follow the trajectory of the fiber bundles, referred to as outliers, were removed. Hence, this framework facilitates the estimation of a connectome with geometrically consistent streamlines, as outlier removal potentially leads to a reduction of FP bundles/connections.

Machine learning methods

Advanced machine learning-based tractography algorithms have also demonstrated superior performance in comparison to the conventional tractography algorithms for mapping connectomes. Neher and colleagues proposed the first machine learning algorithm for deterministic tractography [143], where the study utilized a random forest to learn a mapping between raw diffusion measurements and fiber direction to generate streamlines. A voting process among the fiber directions in a local neighborhood of the current streamline position provided a single direction in which the streamline proceeded. The method was successful in generating more VCs than conventional tractography algorithms.

A feed-forward recurrent network [144] and a multilayer perceptron [145] also mapped the raw diffusion measurements to local streamline orientations which not only used the local measurements but also considered the previous measurements along the extent of a particular streamline. A similar recurrent network was proposed by Benou and Raviv [146], where the model predicted a probabilistic estimation of the local fiber orientation distribution, instead of a deterministic fiber direction. These methods outperformed most tractography algorithms submitted to ISMRM 2015 Tractography Challenge for the *Tractometer* evaluation metrics.

A block-decomposition and stitching algorithm is another connectome mapping algorithm based on deep learning, but the framework could also be used as a simple augmentation to enhance the accuracy of connectome mapped using conventional tractography [147]. The framework involved decomposing the dMRI into overlapping blocks. Later, the local connectivity matrices were estimated for each block either using deep learning or tractography. This local connectivity served as buildings blocks used to stitch together the overlapping blocks, thereby yielding a whole-brain connectivity matrix. The study reported that block decomposition can improve the accuracy of connectivity matrix reconstruction by up to 30%, relative to the best performing streamline tractography algorithm [148]. This improvement was due to the robustness to noise and PVE that was achieved due to the redundancy introduced by allowing blocks to overlap.

7. Discussion:

dMRI-based tractography was originally developed to virtually dissect WM tracts [149]. The estimated fiber tracts were later used to map connectomes which are primarily concerned with the absence or presence of a fiber bundle between a pair of brain regions and their strength. The geometrical properties (curvature, trajectory, or spatial extent) of the reconstructed fiber bundles are typically not utilized when mapping connectomes. Therefore, evaluating tractography performance based on geometrically consistent fiber bundles does not guarantee an accurate connectome reconstruction. For a comprehensive discussion on the limitations of tractography, refer to [66].

Limitations of validation phantoms/maps

In the absence of the "ground truth" of the human brain, three types of validation methods have been utilized in the literature for evaluating fiber orientation estimation, tractography, and connectomes. But these methods have drawbacks and limitations. For tracer maps, a limited number of regions can be analyzed, where the integrity of the study is dependent on the type of tracer [150]. The tracer maps offer a mismatch in the spatial resolution with dMRI, which complicates the comparison between the two modalities. Furthermore, the tracer maps are generated from heterogeneous sources (different species of monkeys or mice), therefore building a normative ground truth is difficult and challenging. The invasive

nature of tracer methods makes it impossible to study the *in vivo* characteristics of a human brain. Thus, the conclusion drawn from tracer studies in animals does not guarantee the success of tractography for the human brain due to substantial differences in their anatomies *e.g.* macaque neocortex is ≈10 fold smaller than a human [119].

Physical phantoms overcome the invasive nature of tracer maps but the characteristics of the synthetic fibers used for constructing these phantoms have shown dissimilarity with real tissues [82, 151]. Furthermore, only a limited number of fibers can be modeled for physical phantoms, whose geometrical complexity is much less than a human brain. On the other hand, numerical phantoms provide better control of generating fiber tracts in comparison to physical phantoms, as complex interdigitating fibers under varying acquisition conditions (SNR, diffusion-weighted gradients and b-value) can be simulated in the absence of real data acquisition. Physical and numerical phantoms offer a degree of controllability and definability of fiber tracts, but these phantoms lack the realism of physical tissues, true signal noise and artifacts [151]. Thus, the accuracy and precision of the connectome estimated by tractography reported for these methods may not be consistent with the *in vivo* environment [83]. Due to better controllability, availability of computational resources and no requirement for real acquisitions, numerical phantoms are used extensively for evaluating tractography. Regardless of the limitation and challenges of these validation methods, phantoms provide an important tool to evaluate local diffusion models, tractography and connectomes.

Tractography parameters control the accuracy of connectome

The validation studies have reported that the accuracy of the estimated connectomes depends on many factors which include (i) selection of fiber/diffusion estimation model, (ii) tractography algorithms, (iii) tractography control parameters like angle threshold, seeding methodology and stopping criteria, (iv) parcellation scheme and (v) evaluation criteria (*e.g.* binary or weighted connectivity matrix, evaluation metric like TPR, FPR, correlation coefficient or network analysis).

Due to the methodological differences in the orientation estimation model and tractography algorithms to address the complex microstructural properties of the brain, it is not surprising that the accuracy of connectome reconstruction varies. Moreover, tractography algorithms depend on user-defined control parameters whose optimal values are generally unknown. Hence, it is expected that the connectomes estimated under varying values of these parameters are not consistent [57, 105, 129, 135, 152]. But the validation studies have demonstrated that the appropriate combination of these control parameters can recover a connectome with high sensitivity, but high specificity of the connectome is not always guaranteed. The Tractometer study demonstrated that for the "FiberCup" phantom comprising only 7 fiber bundles, tractography algorithms yielded more ICs/IBs than VCs/VB (ratio VC/VC+IC < 50% and IBs>7) under different combinations of control parameters [57].

The variation in tractography parameters was also systematically evaluated against the tracer extracted mice connectome, where relaxing the stopping criteria (low FOD threshold) and angle threshold increased both TPR and FPR [105]. The reconstructed connectomes also varied for different seeding methodologies [57, 131], where seeding throughout the WM volume can result in over-sampling of long fiber bundles. This oversampling can potentially lead to overestimation of connectivity strengths for long connections. On the other hand, initiating streamline tracking from the WM/GM interface can underestimate the connectivity of long connections, due to the inherent difficulties in propagating streamlines over long distances [153]. Thus, the selection of the optimal tractography parameters depends on the trade-off between sensitivity and specificity. It should also be noted that control parameters are dependant on the tractography algorithm (deterministic, probabilistic, and global).

Accuracy of connectome varies with brain parcellation scheme

The choice of parcellation scheme is also critical in constructing a reliable connectome. It is well-known that the performance of the reconstructed connectomes varies with the resolution of the cortical parcellation [154]. Generally, connectomes are reproducible when mapped using parcellation with fewer nodes, but more details could be preserved for parcellation with finer subdivisions [122]. The agreement between the tracer map and tractography reconstructed connectome is higher for parcellation with low-resolution than high-resolution [100]. The selection of a parcellation scheme is usually not obvious and depends on a given application. Systematic evaluation of the impact of the coarseness of parcellation on mapping connectome may help in understanding the inconstancies in their accuracy.

Local orientation models and tractography are inherently limited

In addition to the beforementioned factors, the current local orientation models and tractography are unable to provide an accurate structural map of the human brain [109]. The estimation of connectome depends on the microstructural properties of the tissues, where the complex fiber configurations remain a bottleneck for state-of-the art tractography algorithms. It is expected that tractography can provide better results for high-quality dMRI datasets. Surprisingly, Thomas and colleagues [54]) did not observe an improvement in the performance of the reconstructed connectome for the exceptional high-quality dMRI (high SNR and spatial resolution of 250 μm). The ISMRM 2015 Tractography Challenge also supported this finding where high-resolution data did not reduce the number of FPs [133], although improvement in the spatial properties of the fiber bundles was observed. Schilling and colleagues [155] demonstrated that the prevalence of crossing fibers increased with an increase in spatial resolution. Similarly, reconstruction of different brain networks of the same subjects was observed for dMRI acquired at different magnetic fields (7T-higher SNR and 3T-lower SNR) [156] and different scanning parameters [157]. Hence, high-quality

imaging can improve the performance of tractography, but development of novel algorithms is also needed to address the inherent limitations of current fiber orientations models and tractography algorithms.

False connections are inevitable

Apart from the variation in the connectome accuracy for different orientation estimation models, tractography algorithms and its control parameter, another common consensus among connectome evaluation studies is the estimation of false connections. The generation of FP is inevitable, regardless of the tractography algorithms and the selection of optimal control parameters. In the ISMRM 2015 Tractography Challenge, the submitted tractograms contained an average of 88 ± 58 IBs where the ground-truth phantoms comprised only 25 bundles [132]. The sensitivity and specificity also varied for different tractography algorithms. Deterministic tractography algorithms have shown lower sensitivity and higher specificity in comparison to probabilistic algorithms. Probabilistic tractography is better at estimating true connections with geometrical accuracy (high value of average bundle coverage) but at the expense of a high number of false connections [57]. The connectome mapping performance of probabilistic algorithms could be improved by selecting optimal tractography parameters and discarding connections with fewer streamlines (streamline threshold) [148].

Advanced methods are effective

The reduction in false connections remains an open challenge. The inclusion of microstructural properties to filter the false streamlines can potentially reduce the false connections, as demonstrated by many filtering algorithms [136, 138-140]. The common goal of filtering techniques is to reduce the signal prediction error to reduce the bias in the generated tractograms. A significant improvement in the reduction of the false connections was demonstrated by a recent study COMMIT2 [141] that not only utilized the microstructural properties of WM but also included anatomical priors computed using tractogram segmentation. Bundle segmentation involves integration of anatomical knowledge and constraints on the inclusion/exclusion of the ROIs during and post-tracking of the streamlines. Schilling and colleagues [158] demonstrated that bundle segmentation can improve the accuracy of reconstructed connectomes in comparison to the unconstrained application of tractography algorithms. For example, integration of anatomical priors in the form of segmented bundles led to improvement of COMMIT2.

Moreover, advanced machine learning-based tractography algorithms have also demonstrated potential in estimating accurate connectomes [143, 144]. Integrating functional information into the connectome mapping process using imaging modalities such as functional MRI can also aid in improving the accuracy of the reconstructed connectome [159].

Common findings of validation studies

i. **Conclusions:**
   - The accuracy of the connectomes is similar for phantoms with low FA values (≈0.1), regardless of the fiber orientation models and tractography algorithms
   - The performance of tractography is dependent on the choice of algorithm (deterministic, probabilistic or global) and associated user-defined control parameters
   - The choice of the parcellation scheme affects the accuracy of a connectome
   - Probabilistic tractography does not provide a higher correlation with the ground-truth in comparison to deterministic methods.
   - False connections are inevitable for mapping connectomes
   - High sensitivity and high specificity for a tractography estimated connectome is not yet achievable

ii. **Recommendations:**
   - Multi-fiber estimation model is preferred over the tensor model
   - Post-processing of the reconstructed tractogram is recommended to remove false connections
   - Introducing anatomical priors and constraints on tractography can improve the accuracy of connectomes
   - Probabilistic tractography is recommended for the cases where accuracy of the geometrical properties of the estimated connections is required

Connectome evaluation criteria needs standardization

Most studies have analyzed binary connectomes, ignoring the strength of connections [56, 57, 141, 148]. Fewer studies have used the number of streamlines and the volume of the fiber bundles to quantify the connection strength, but it remains an open challenge to evaluate the connectivity strength of the estimated fiber bundles. Moreover, there does not exist any phantom that primarily addressed the connectivity strength of the underlying connections. Even for binary connectomes, there does not exist a standard evaluation method for comparing connectomes. Different performance metrics were used to evaluate the performance of connectomes, which limits the comparison between different studies. Recent studies have used Tractometer evaluation metrics to report the accuracy of the estimated connectomes, where variation in the accuracy of connectomes was reported for different tractography algorithms [56, 57]. On the other hand, the connectome mapping capability of deterministic tensor, probabilistic CSD and global tractography for rat brains were found to be similar when Jaccard index was used as an evaluation metric [106]. Hence, the evaluation criteria play an important role in validating the connectome. Standardizing the evaluation

process is also an ultimate need to facilitate the fair comparison of various tractography algorithms and results from different studies.

The current validation studies involved comparative analysis where one algorithm outperformed the other. But so far no evaluation criteria could be found in the literature that could be used as a standard optimal performance for tractography algorithms. For example, Zalesky and colleagues have recommended the 2:1 rule of thumb for connectomes [160] *i.e.* the FNs should be twice the number of FPs. Such rules can help in screening current and developing new tractography algorithms with optimal performance.

Potential research directions

The focus of the current phantoms is on modeling the microstructural properties of a healthy brain. Although it is expected that the reliable performance of a tractography algorithm for a healthy brain could be trusted for studying neurological disorders. But so far, no phantom has been developed that modeled brain regions with pathologies. This is important not only to validate tractography for identifying the regions affected by pathology that might lead to FPs but also for evaluating streamline filtering algorithms. The filtering algorithms rely on the local microstructural properties which vary for local normal and pathology affected regions. This behavior could adversely affect the filtering process spuriously discarding the streamlines for regions with pathology.

Although tractography can reconstruct valid fiber bundles, we need to revisit local orientation estimation and tractography to improve the accuracy of the connectome reconstruction. The local orientation estimation models need enhancement to resolve more acute angles for conditions where multiple fasciculi converge toward a small region and diverge afterward [120]. Moreover, tractography is fundamentally ill-posed, where even computationally expensive global tractography utilizes local voxel-wise information and hence it inherently generates FPs [132]. It should also be noted that the spatial disparity between axonal structures (submillimeter) and typical voxel size (1-2mm) also imposes limits on fiber bundle estimation, where even ultra-high field MRI cannot adequately quantify the number of axonal elements per voxel area [161]. Hence, novel methodological and hardware advancements are needed to improve the performance of tractography algorithms.

Summary:

In this paper, we reviewed the studies that have evaluated the connectomes estimated by tractography algorithms. Connectome mapping involves identifying the fiber bundles connecting pairs of regions, thus the accurate geometrical reconstruction of the fiber bundles does not guarantee a generation of an accurate connectome. This highlights the importance of the connectome evaluation process. In the absence of the "ground-truth" of the human brain,

three types of validation methods (tracer maps, physical and numerical) have been utilized for evaluating fiber orientation estimation, tractography and connectomes.

There is a consensus between these studies that the current tractography algorithms can reconstruct a substantial number of true connections encapsulated in the phantoms. But the performance of the algorithms is dependent on the selection of tractography parameters and the algorithm itself. The accuracy of the connectomes varies for the tractography algorithm, where probabilistic tractography algorithms are prone to more false connections, compared to deterministic variants. The performance of the generated connectome can be improved by utilizing the microstructural and anatomical priors to filter the streamlines that are biologically infeasible. Such filtering algorithms and advanced machine learning methods have demonstrated great potential in improving the accuracy of connectomes. Thus, the new tractography or connectome reconstruction methods should focus on controlling the generation of false connections during the fiber bundle estimation process.

Appendix:

Table A1: Local orientation estimation models and tractography algorithms

	Model/Algorithm	Explanation
Local Orientation Estimation	Tensor [7]	A 3x3 symmetric and positive definite covariance matrix, which describes the covariances of diffusion displacements along the three perpendicular directions, yielding a principal diffusion direction in each voxel
	Multi-tensor [162]	Extension of tensor model to account for multiple fiber populations
	Diffusion Spectrum Imaging-DSI [18]	Estimates the spin displacement probability density function (PDF) using an inverse Fourier transform of the modulus of the measured signal, where the q-space is sampled on 3D Cartesian grid
	Q-ball Imaging – QBI or Q-ball [14-16, 163]	Unlike DSI, the q-space is sampled on a sphere to approximate the diffusion orientation distribution function (dODF) The model has been optimized using the spherical harmonic basis
	Constrained Spherical Deconvolution - CSD [8, 9]	Assumes that the diffusion-weighted signal can be expressed as the convolution over a unit sphere of the response function (the signal attenuation for a single fiber population) with the fiber ODF (FOD). Hence, the FOD within the voxel can therefore be computed using spherical deconvolution
	Persistent Angular Structure - PAS [164]	A special case of spherical deconvolution, which models the intravoxel diffusion using a discrete number of fiber compartments [165, 166]
	Generalized Q-sampling Imaging - GQI [167]	Estimates spin distribution function (SDF) which represents a quantitative distribution of the spins undergoing diffusion. It uses Fourier transforms to produce SDF from QBI or DSI [168]

	Compartment-based fiber-orientation distribution function (FOD) model [169]	Integrates the spherical deconvolution framework for FOD estimation with compartment models of water diffusion based on the underlying microstructure of brain tissues
	Ball and stick model [26]	Models axons as impermeable cylinders of a single radius and isotropic diffusion outside the axon in the extracellular compartments [170]
Tractography	Deterministic [20, 23, 171-174]	Generates streamlines or fiber trajectories stepwise following the principal diffusion direction
	Probabilistic [26, 175-177]	Generates streamlines in a stepwise manner but the propagation direction does not necessarily follow the principal fiber direction. Instead, the ODF is sampled probabilistically to determine the direction of streamline propagation.
	Global [33, 35, 38, 178, 179]	Assumes that fiber trajectories are represented by paths of highest diffusion. A large ensemble of streamlines is generated, where each streamline is then used to synthesize the diffusion signal. The synthesized signal is compared with the measured dMRI signal and the difference is progressively minimized via optimization.

References:

1. Hagmann, P., et al., *Mapping human whole-brain structural networks with diffusion MRI.* PloS one, 2007. **2**(7): p. e597.
2. Hagmann, P., et al., *Mapping the structural core of human cerebral cortex.* PLoS biology, 2008. **6**(7): p. e159.
3. Sporns, O., G. Tononi, and R. Kötter, *The human connectome: a structural description of the human brain.* PLoS computational biology, 2005. **1**(4).
4. Gatto, R.G. and T. Asakawa, *New molecular insights, innovative technologies, and medical approaches in the "Exploration of mechanisms in cortical plasticity".* Journal of Integrative Neuroscience, 2020. **19**(4): p. 733-734.
5. Hamaide, J., G. De Groof, and A. Van der Linden, *Neuroplasticity and MRI: a perfect match.* NeuroImage, 2016. **131**: p. 13-28.
6. Basser, P.J., J. Mattiello, and D. LeBihan, *MR diffusion tensor spectroscopy and imaging.* Biophysical journal, 1994. **66**(1): p. 259-267.
7. Basser, P.J., J. Mattiello, and D. LeBihan, *Estimation of the effective self-diffusion tensor from the NMR spin echo.* Journal of Magnetic Resonance, Series B, 1994. **103**(3): p. 247-254.
8. Tournier, J.-D., et al., *Direct estimation of the fiber orientation density function from diffusion-weighted MRI data using spherical deconvolution.* NeuroImage, 2004. **23**(3): p. 1176-1185.
9. Tournier, J.-D., F. Calamante, and A. Connelly, *Robust determination of the fibre orientation distribution in diffusion MRI: non-negativity constrained super-resolved spherical deconvolution.* Neuroimage, 2007. **35**(4): p. 1459-1472.
10. Jeurissen, B., et al., *Multi-tissue constrained spherical deconvolution for improved analysis of multi-shell diffusion MRI data.* NeuroImage, 2014. **103**: p. 411-426.

11. Alexander, D.C. *Maximum entropy spherical deconvolution for diffusion MRI*. in *Biennial International Conference on Information Processing in Medical Imaging*. 2005. Springer.
12. Schultz, T., C.-F. Westin, and G. Kindlmann. *Multi-diffusion-tensor fitting via spherical deconvolution: a unifying framework*. in *International Conference on Medical Image Computing and Computer-Assisted Intervention*. 2010. Springer.
13. Canales-Rodríguez, E.J., L. Melie-García, and Y. Iturria-Medina, *Mathematical description of q-space in spherical coordinates: exact q-ball imaging.* Magnetic Resonance in Medicine: An Official Journal of the International Society for Magnetic Resonance in Medicine, 2009. **61**(6): p. 1350-1367.
14. Descoteaux, M., et al., *Regularized, fast, and robust analytical Q-ball imaging.* Magnetic Resonance in Medicine: An Official Journal of the International Society for Magnetic Resonance in Medicine, 2007. **58**(3): p. 497-510.
15. Tuch, D.S., *Q-ball imaging.* Magnetic Resonance in Medicine, 2004. **52**(6): p. 1358-1372.
16. Hess, C.P., et al., *Q-ball reconstruction of multimodal fiber orientations using the spherical harmonic basis.* Magnetic Resonance in Medicine: An Official Journal of the International Society for Magnetic Resonance in Medicine, 2006. **56**(1): p. 104-117.
17. Aganj, I., C. Lenglet, and G. Sapiro. *ODF reconstruction in q-ball imaging with solid angle consideration*. in *Biomedical Imaging: From Nano to Macro, 2009. ISBI'09. IEEE International Symposium on*. 2009. IEEE.
18. Wedeen, V.J., et al., *Mapping complex tissue architecture with diffusion spectrum magnetic resonance imaging.* Magnetic resonance in medicine, 2005. **54**(6): p. 1377-1386.
19. Wedeen, V.J., et al., *Diffusion spectrum magnetic resonance imaging (DSI) tractography of crossing fibers.* NeuroImage, 2008. **41**: p. 1267-1277.
20. Mori, S., et al., *Three-dimensional tracking of axonal projections in the brain by magnetic resonance imaging.* Annals of Neurology: Official Journal of the American Neurological Association and the Child Neurology Society, 1999. **45**(2): p. 265-269.
21. Basser, P.J., et al., *In vivo fiber tractography using DT-MRI data.* Magnetic resonance in medicine, 2000. **44**(4): p. 625-632.
22. Basser, P.J. *Fiber-tractography via diffusion tensor MRI (DT-MRI)*. in *Proceedings of the 6th Annual Meeting ISMRM, Sydney, Australia*. 1998.
23. Tournier, J.D., F. Calamante, and A. Connelly, *MRtrix: diffusion tractography in crossing fiber regions.* International Journal of Imaging Systems and Technology, 2012. **22**(1): p. 53-66.
24. Conturo, T.E., et al., *Tracking neuronal fiber pathways in the living human brain.* Proceedings of the National Academy of Sciences, 1999. **96**(18): p. 10422-10427.
25. Yeh, F.-C., et al., *Deterministic diffusion fiber tracking improved by quantitative anisotropy.* PloS one, 2013. **8**(11): p. e80713.
26. Behrens, T.E., et al., *Probabilistic diffusion tractography with multiple fibre orientations: What can we gain?* Neuroimage, 2007. **34**(1): p. 144-155.
27. Tournier, J.D., F. Calamante, and A. Connelly. *Improved probabilistic streamlines tractography by 2nd order integration over fibre orientation distributions*. in *Proceedings of the international society for magnetic resonance in medicine*. 2010.
28. Descoteaux, M., et al., *Deterministic and probabilistic tractography based on complex fibre orientation distributions.* IEEE transactions on medical imaging, 2009. **28**(2): p. 269-286.
29. Friman, O., G. Farneback, and C.-F. Westin, *A Bayesian approach for stochastic white matter tractography.* IEEE transactions on medical imaging, 2006. **25**(8): p. 965-978.

30. Zhang, M., K.E. Sakaie, and S.E. Jones, *Logical foundations and fast implementation of probabilistic tractography.* IEEE transactions on medical imaging, 2013. **32**(8): p. 1397-1410.
31. Aganj, I., et al., *A Hough transform global probabilistic approach to multiple-subject diffusion MRI tractography.* Medical image analysis, 2011. **15**(4): p. 414-425.
32. Fillard, P., C. Poupon, and J.-F. Mangin. *A novel global tractography algorithm based on an adaptive spin glass model*. in *International conference on medical image computing and computer-assisted intervention*. 2009. Springer.
33. Jbabdi, S., et al., *A Bayesian framework for global tractography.* Neuroimage, 2007. **37**(1): p. 116-129.
34. Lemkaddem, A., et al., *Global tractography with embedded anatomical priors for quantitative connectivity analysis.* Frontiers in neurology, 2014. **5**: p. 232.
35. Mangin, J.-F., et al., *Toward global tractography.* Neuroimage, 2013. **80**: p. 290-296.
36. Reisert, M., et al., *Disentangling micro from mesostructure by diffusion MRI: A Bayesian approach.* Neuroimage, 2017. **147**: p. 964-975.
37. Yamada, M., et al., *Diffusion-tensor neuronal fiber tractography and manganese-enhanced MR imaging of primate visual pathway in the common marmoset: preliminary results.* Radiology, 2008. **249 3**: p. 855-64.
38. Reisert, M., et al., *Global fiber reconstruction becomes practical.* Neuroimage, 2011. **54**(2): p. 955-962.
39. Jones, D.K., T.R. Knösche, and R. Turner, *White matter integrity, fiber count, and other fallacies: the do's and don'ts of diffusion MRI.* Neuroimage, 2013. **73**: p. 239-254.
40. Knösche, T.R., et al., *Validation of tractography: comparison with manganese tracing.* Human brain mapping, 2015. **36**(10): p. 4116-4134.
41. Caruyer, E., et al. *A comparative study of 16 tractography algorithms for the corticospinal tract: reproducibility and subject-specificity*. in *Proceedings of the International Society for Magnetic Resonance in Medicine... Scientific Meeting and Exhibition. International Society for Magnetic Resonance in Medicine. Scientific Meeting and Exhibition*. 2014. NIH Public Access.
42. Lazar, M., K. Hasan, and A. Alexander. *Bootstrap analysis of DT-MRI tractography techniques: streamlines and tensorlines*. in *Proc 9th ISMRM Annual Meeting, Glasgow*. 2001.
43. Zhan, L., et al., *Comparison of nine tractography algorithms for detecting abnormal structural brain networks in Alzheimer's disease.* Frontiers in Aging Neuroscience, 2015. **7**(48).
44. Fieremans, E. and H.-H. Lee, *Physical and numerical phantoms for the validation of brain microstructural MRI: A cookbook.* NeuroImage, 2018. **182**: p. 39-61.
45. von dem Hagen, E.A. and R.M. Henkelman, *Orientational diffusion reflects fiber structure within a voxel.* Magnetic Resonance in Medicine: An Official Journal of the International Society for Magnetic Resonance in Medicine, 2002. **48**(3): p. 454-459.
46. Lin, C.-P., et al., *Validation of diffusion spectrum magnetic resonance imaging with manganese-enhanced rat optic tracts and ex vivo phantoms.* Neuroimage, 2003. **19**(3): p. 482-495.
47. Cho, K.-H., et al., *Evaluation of the accuracy and angular resolution of q-ball imaging.* Neuroimage, 2008. **42**(1): p. 262-271.
48. Poupon, C., et al., *New diffusion phantoms dedicated to the study and validation of high-angular-resolution diffusion imaging (HARDI) models.* Magnetic Resonance in Medicine:

An Official Journal of the International Society for Magnetic Resonance in Medicine, 2008. **60**(6): p. 1276-1283.
49. Zhan, W. and Y. Yang, *How accurately can the diffusion profiles indicate multiple fiber orientations? A study on general fiber crossings in diffusion MRI.* Journal of Magnetic Resonance, 2006. **183**(2): p. 193-202.
50. Daducci, A., et al., *Quantitative comparison of reconstruction methods for intra-voxel fiber recovery from diffusion MRI.* IEEE transactions on medical imaging, 2014. **33**(EPFL-ARTICLE-183667): p. 384-399.
51. Dyrby, T.B., et al., *Validation of in vitro probabilistic tractography.* NeuroImage, 2007. **37**: p. 1267-1277.
52. Scifo, P., et al. *A dedicated phantom for diffusion tensor imaging studies*. in *Proc. Int. Soc. Magn. Reson. Med*. 2004.
53. Moldrich, R.X., et al., *Comparative mouse brain tractography of diffusion magnetic resonance imaging.* Neuroimage, 2010. **51**(3): p. 1027-1036.
54. Thomas, C., et al., *Anatomical accuracy of brain connections derived from diffusion MRI tractography is inherently limited.* Proceedings of the National Academy of Sciences of the United States of America, 2014. **111 46**: p. 16574-9.
55. Tournier, J., F. Calamante, and A. Connelly. *Effect of step size on probabilistic streamlines: implications for the interpretation of connectivity analysis*. in *Proc. Intl. Soc. Mag. Reson. Med*. 2011.
56. Neher, P.F., et al., *Strengths and weaknesses of state of the art fiber tractography pipelines–a comprehensive in-vivo and phantom evaluation study using tractometer.* Medical image analysis, 2015. **26**(1): p. 287-305.
57. Côté, M.-A., et al., *Tractometer: towards validation of tractography pipelines.* Medical image analysis, 2013. **17**(7): p. 844-857.
58. Girard, G., et al., *Towards quantitative connectivity analysis: reducing tractography biases.* Neuroimage, 2014. **98**: p. 266-278.
59. Tournier, J.-D., F. Calamante, and A. Connelly, *Determination of the appropriate b value and number of gradient directions for high-angular-resolution diffusion-weighted imaging.* NMR in biomedicine, 2013. **26 12**: p. 1775-86.
60. Tournier, J.-D., et al., *Resolving crossing fibres using constrained spherical deconvolution: validation using diffusion-weighted imaging phantom data.* Neuroimage, 2008. **42**(2): p. 617-625.
61. Lazar, M. and A.L. Alexander, *An error analysis of white matter tractography methods: synthetic diffusion tensor field simulations.* NeuroImage, 2003. **20**: p. 1140-1153.
62. Koch, M.A., D.G. Norris, and M. Hund-Georgiadis, *An investigation of functional and anatomical connectivity using magnetic resonance imaging.* Neuroimage, 2002. **16**(1): p. 241-250.
63. Zhang, Z., et al., *Altered functional–structural coupling of large-scale brain networks in idiopathic generalized epilepsy.* Brain, 2011. **134**(10): p. 2912-2928.
64. Camchong, J., et al., *Altered functional and anatomical connectivity in schizophrenia.* Schizophrenia bulletin, 2011. **37**(3): p. 640-650.
65. Gatto, R.G., et al., *Detection of axonal degeneration in a mouse model of Huntington's disease: comparison between diffusion tensor imaging and anomalous diffusion metrics.* Magnetic Resonance Materials in Physics, Biology and Medicine, 2019. **32**(4): p. 461-471.

66. Schilling, K.G., et al., *Challenges in diffusion MRI tractography–Lessons learned from international benchmark competitions.* Magnetic resonance imaging, 2018.
67. Sotiropoulos, S.N. and A. Zalesky, *Building connectomes using diffusion MRI: why, how and but.* NMR in Biomedicine, 2019. **32**(4): p. e3752.
68. Ning, L., et al., *Sparse Reconstruction Challenge for diffusion MRI: Validation on a physical phantom to determine which acquisition scheme and analysis method to use?* Medical image analysis, 2015. **26 1**: p. 316-31.
69. Bassett, D.S. and E.T. Bullmore, *Human brain networks in health and disease.* Current opinion in neurology, 2009. **22**(4): p. 340.
70. Zalesky, A., et al., *Disrupted axonal fiber connectivity in schizophrenia.* Biological psychiatry, 2011. **69**(1): p. 80-89.
71. Ciccarelli, O., et al., *Diffusion-based tractography in neurological disorders: concepts, applications, and future developments.* The Lancet Neurology, 2008. **7**(8): p. 715-727.
72. Casey, B., et al., *Imaging the developing brain: what have we learned about cognitive development?* Trends in cognitive sciences, 2005. **9**(3): p. 104-110.
73. Bressler, S.L. and V. Menon, *Large-scale brain networks in cognition: emerging methods and principles.* Trends in cognitive sciences, 2010. **14**(6): p. 277-290.
74. Khundrakpam, B.S., et al., *Developmental changes in organization of structural brain networks.* Cerebral Cortex, 2012. **23**(9): p. 2072-2085.
75. Tamnes, C.K., et al., *Diffusion MRI of white matter microstructure development in childhood and adolescence: Methods, challenges and progress.* Developmental cognitive neuroscience, 2018. **33**: p. 161-175.
76. Keenan, K.E., et al., *Quantitative magnetic resonance imaging phantoms: A review and the need for a system phantom.* Magnetic resonance in medicine, 2018. **79**(1): p. 48-61.
77. DeWerd, L.A. and M. Kissick, *The phantoms of medical and health physics*. 2014: Springer.
78. Does, M.D., *Inferring brain tissue composition and microstructure via MR relaxometry.* NeuroImage, 2018. **182**: p. 136-148.
79. Novikov, D.S., et al., *Quantifying brain microstructure with diffusion MRI: Theory and parameter estimation.* NMR in Biomedicine, 2016: p. e3998.
80. Panagiotaki, E., et al., *Compartment models of the diffusion MR signal in brain white matter: a taxonomy and comparison.* Neuroimage, 2012. **59**(3): p. 2241-2254.
81. Yanasak, N. and J. Allison, *Use of capillaries in the construction of an MRI phantom for the assessment of diffusion tensor imaging: demonstration of performance.* Magnetic resonance imaging, 2006. **24**(10): p. 1349-1361.
82. Perrin, M., et al., *Validation of q-ball imaging with a diffusion fibre-crossing phantom on a clinical scanner.* Philosophical Transactions of the Royal Society of London B: Biological Sciences, 2005. **360**(1457): p. 881-891.
83. Pullens, P., A. Roebroeck, and R. Goebel, *Ground truth hardware phantoms for validation of diffusion-weighted MRI applications.* Journal of Magnetic Resonance Imaging, 2010. **32**(2): p. 482-488.
84. Lorenz, R., et al., *Anisotropic phantoms for quantitative diffusion tensor imaging and fiber-tracking validation.* Applied Magnetic Resonance, 2008. **33**(4): p. 419.
85. Farrher, E., et al., *Novel multisection design of anisotropic diffusion phantoms.* Magnetic resonance imaging, 2012. **30**(4): p. 518-526.

86. Campbell, J.S., et al. *Validation and regularization in diffusion MRI tractography*. in *3rd IEEE International Symposium on Biomedical Imaging: Nano to Macro, 2006.* 2006. IEEE.
87. Fillard, P., et al., *Quantitative evaluation of 10 tractography algorithms on a realistic diffusion MR phantom.* Neuroimage, 2011. **56**(1): p. 220-234.
88. Neher, P.F., et al., *Fiberfox: facilitating the creation of realistic white matter software phantoms.* Magnetic resonance in medicine, 2014. **72 5**: p. 1460-70.
89. Sato, K., et al., *Understanding microstructure of the brain by comparison of neurite orientation dispersion and density imaging (NODDI) with transparent mouse brain.* Acta Radiologica Open, 2017. **6**(4): p. 2058460117703816.
90. Ianuş, A., et al., *Accurate estimation of microscopic diffusion anisotropy and its time dependence in the mouse brain.* Neuroimage, 2018. **183**: p. 934-949.
91. Schmahmann, J.D., et al., *Association fibre pathways of the brain: parallel observations from diffusion spectrum imaging and autoradiography.* Brain, 2007. **130 Pt 3**: p. 630-53.
92. Gatto, R.G., et al., *In vivo diffusion MRI detects early spinal cord axonal pathology in a mouse model of amyotrophic lateral sclerosis.* NMR in Biomedicine, 2018. **31**(8): p. e3954.
93. Harsan, L.-A., et al., *Mapping remodeling of thalamocortical projections in the living reeler mouse brain by diffusion tractography.* Proceedings of the National Academy of Sciences, 2013. **110**(19): p. E1797-E1806.
94. Aung, W.Y., S. Mar, and T.L. Benzinger, *Diffusion tensor MRI as a biomarker in axonal and myelin damage.* Imaging in medicine, 2013. **5**(5): p. 427.
95. Klingler, J. and E. Ludwig, *Atlas cerebri humani: der innere Bau des Gehirns dargestellt auf Grund makroskopischer Präparate: the inner structure of the brain demonstrated on the basis of macroscopical preparations: la structure interne du cerveau démontrée sur des préparations macroscopiques: la arquitectura interna del cerebro demostrada mediante preparaciones macroscópicas*. 1956: Karger Basel.
96. Klingler, J. and P. Gloor, *The connections of the amygdala and of the anterior temporal cortex in the human brain.* Journal of Comparative Neurology, 1960. **115**(3): p. 333-369.
97. Gyengesi, E., et al., *Semi-automated 3D segmentation of major tracts in the rat brain: comparing DTI with standard histological methods.* Brain Structure and Function, 2014. **219**(2): p. 539-550.
98. Reveley, C., et al., *Superficial white matter fiber systems impede detection of long-range cortical connections in diffusion MR tractography.* Proceedings of the National Academy of Sciences of the United States of America, 2015. **112 21**: p. E2820-8.
99. Jitsuishi, T., et al., *White matter dissection and structural connectivity of the human vertical occipital fasciculus to link vision-associated brain cortex.* Scientific reports, 2020. **10**(1): p. 1-14.
100. Gao, Y., et al., *Validation of DTI tractography-based measures of primary motor area connectivity in the squirrel monkey brain.* PloS one, 2013. **8**(10): p. e75065.
101. van den Heuvel, M.P., et al., *Comparison of diffusion tractography and tract-tracing measures of connectivity strength in rhesus macaque connectome.* Human brain mapping, 2015. **36**(8): p. 3064-3075.
102. Donahue, C.J., et al., *Using diffusion tractography to predict cortical connection strength and distance: a quantitative comparison with tracers in the monkey.* Journal of Neuroscience, 2016. **36**(25): p. 6758-6770.

103. Calabrese, E., et al., *A diffusion MRI tractography connectome of the mouse brain and comparison with neuronal tracer data.* Cerebral cortex, 2015. **25**(11): p. 4628-4637.
104. Hubbard, P.L. and G.J. Parker, *Validation of tractography*, in *Diffusion MRI*. 2014, Elsevier. p. 453-480.
105. Aydogan, D.B., et al., *When tractography meets tracer injections: a systematic study of trends and variation sources of diffusion-based connectivity.* Brain Structure and Function, 2018. **223**: p. 2841-2858.
106. Sinke, M.R., et al., *Diffusion MRI-based cortical connectome reconstruction: dependency on tractography procedures and neuroanatomical characteristics.* Brain Structure and Function, 2018: p. 1-17.
107. Kötter, R., *Online retrieval, processing, and visualization of primate connectivity data from the CoCoMac Database.* Neuroinformatics, 2004. **2**: p. 127-144.
108. Hagmann, P., et al. *Quantitative validation of MR tractography using the CoCoMac database*. in *ISMRM 2008, 16th Scientific Meeting of the International Society for Magnetic Resonance in Medicine*. 2008.
109. Thomas, C., et al., *Anatomical accuracy of brain connections derived from diffusion MRI tractography is inherently limited.* Proceedings of the National Academy of Sciences, 2014. **111**(46): p. 16574-16579.
110. Seehaus, A.K., et al., *Histological validation of DW-MRI tractography in human postmortem tissue.* Cerebral cortex, 2012. **23**(2): p. 442-450.
111. Azadbakht, H., et al. *Validation of tractography against in vivo tracing in the macaque visual system: effect of distance correction*. in *20th Annual Meeting and Exhibition of the International Society for Magnetic Resonance in Medicine (ISMRM 2012)*. 2012.
112. Azadbakht, H., et al., *Validation of high-resolution tractography against in vivo tracing in the macaque visual cortex.* Cerebral Cortex, 2015. **25**(11): p. 4299-4309.
113. Zakszewski, E., et al. *Comparison of probabilistic diffusion tensor tractography with histological tracer studies and RSFC in the rhesus macaque*. in *Proceedings of the 20th Annual Meeting ISMRM*. 2011.
114. Zakszewski, E., et al. *Comparison of probabilistic diffusion tensor tractography and histological tracer studies in the rhesus macaque*. in *International Conference on Medical Image Computing and Computer Assisted Intervention (MICCAI) workshop on Computational Diffusion MRI*. 2011.
115. Loução, R., et al. *Human brain tractography: A DTI vs DKI comparison analysis*. in *2015 IEEE 4th Portuguese Meeting on Bioengineering (ENBENG)*. 2015. IEEE.
116. Glenn, G.R., et al., *Quantitative assessment of diffusional kurtosis anisotropy.* NMR in Biomedicine, 2015. **28**(4): p. 448-459.
117. Wu, Y., et al., *Mitigating gyral bias in cortical tractography via asymmetric fiber orientation distributions.* Medical image analysis, 2020. **59**: p. 101543.
118. Schilling, K.G., et al., *Confirmation of a gyral bias in diffusion MRI fiber tractography.* Human brain mapping, 2018. **39 3**: p. 1449-1466.
119. Donahue, C.J., et al., *Using Diffusion Tractography to Predict Cortical Connection Strength and Distance: A Quantitative Comparison with Tracers in the Monkey.* The Journal of neuroscience, 2016. **36 25**: p. 6758-70.
120. Rheault, F., et al., *Common misconceptions, hidden biases and modern challenges of dMRI tractography.* Journal of neural engineering, 2020. **17**(1): p. 011001.

121. Yeh, C.H., et al., *Mapping structural connectivity using diffusion MRI: Challenges and opportunities.* Journal of Magnetic Resonance Imaging, 2020.
122. Sotiropoulos, S.N. and A. Zalesky, *Building connectomes using diffusion MRI: Why, how and but.* NMR in Biomedicine, 2017: p. e3752.
123. Chen, H., et al., *Optimization of large-scale mouse brain connectome via joint evaluation of DTI and neuron tracing data.* NeuroImage, 2015. **115**: p. 202-213.
124. Glasser, M.F., et al., *The minimal preprocessing pipelines for the Human Connectome Project.* Neuroimage, 2013. **80**: p. 105-124.
125. Tian, Y., et al., *High-resolution connectomic fingerprints: Mapping neural identity and behavior.* NeuroImage, 2021. **229**: p. 117695.
126. Hernandez-Fernandez, M., et al., *Using GPUs to accelerate computational diffusion MRI: From microstructure estimation to tractography and connectomes.* Neuroimage, 2019. **188**: p. 598-615.
127. Colon-Perez, L.M., et al., *Dimensionless, scale invariant, edge weight metric for the study of complex structural networks.* PLOS one, 2015. **10**(7): p. e0131493.
128. Farahani, F.V., W. Karwowski, and N.R. Lighthall, *Application of Graph Theory for Identifying Connectivity Patterns in Human Brain Networks: A Systematic Review.* Frontiers in Neuroscience, 2019. **13**(585).
129. Shen, K., et al., *Exploring the limits of network topology estimation using diffusion-based tractography and tracer studies in the macaque cortex.* NeuroImage, 2019.
130. Haroon, H., et al. *Comparing corticocortical interconnection information from tracer studies and probabilistic tractography in the postmortem macaque brain*. in *ISMRM 16th Scientific Meeting & Exhibition*. 2008.
131. Li, L., et al., *The effects of connection reconstruction method on the interregional connectivity of brain networks via diffusion tractography.* Human brain mapping, 2012. **33 8**: p. 1894-913.
132. Maier-Hein, K.H., et al., *The challenge of mapping the human connectome based on diffusion tractography.* Nature communications, 2017. **8**(1): p. 1349.
133. Côté, M.-A., et al., *Tractometer: Towards validation of tractography pipelines.* Medical image analysis, 2013. **17 7**: p. 844-57.
134. Sarwar, T., K. Ramamohanarao, and A. Zalesky, *Mapping connectomes with diffusion MRI: deterministic or probabilistic tractography?* Magnetic resonance in medicine, 2019. **81 2**: p. 1368-1384.
135. Schilling, K.G., et al., *Limits to anatomical accuracy of diffusion tractography using modern approaches.* NeuroImage, 2019. **185**: p. 1-11.
136. Smith, R.E., et al., *SIFT: Spherical-deconvolution informed filtering of tractograms.* Neuroimage, 2013. **67**: p. 298-312.
137. Smith, R.E., et al., *The effects of SIFT on the reproducibility and biological accuracy of the structural connectome.* Neuroimage, 2015. **104**: p. 253-265.
138. Smith, R.E., et al., *SIFT2: Enabling dense quantitative assessment of brain white matter connectivity using streamlines tractography.* Neuroimage, 2015. **119**: p. 338-351.
139. Pestilli, F., et al., *Evaluation and statistical inference for human connectomes.* Nature methods, 2014. **11**(10): p. 1058.
140. Daducci, A., et al., *COMMIT: convex optimization modeling for microstructure informed tractography.* IEEE transactions on medical imaging, 2014. **34**(1): p. 246-257.

141. Schiavi, S., et al., *A new method for accurate in vivo mapping of human brain connections using microstructural and anatomical information.* Science Advances, 2020. **6**(31): p. eaba8245.
142. Zhang, Z., et al., *Mapping population-based structural connectomes.* NeuroImage, 2018. **172**: p. 130-145.
143. Neher, P.F., et al., *Fiber tractography using machine learning.* Neuroimage, 2017. **158**: p. 417-429.
144. Poulin, P., et al. *Learn to track: Deep learning for tractography*. in *International Conference on Medical Image Computing and Computer-Assisted Intervention (MCCAI)*. 2017. Springer.
145. Wegmayr, V., et al. *Data-driven fiber tractography with neural networks*. in *2018 IEEE 15th International Symposium on Biomedical Imaging (ISBI 2018)*. 2018. IEEE.
146. Benou, I. and T.R. Raviv. *Deeptract: A probabilistic deep learning framework for white matter fiber tractography*. in *International Conference on Medical Image Computing and Computer-Assisted Intervention*. 2019. Springer.
147. Sarwar, T., et al., *Towards deep learning for connectome mapping: A block decomposition framework.* NeuroImage, 2020. **212**: p. 116654.
148. Sarwar, T., K. Ramamohanarao, and A. Zalesky, *Mapping connectomes with diffusion MRI: deterministic or probabilistic tractography?* Magnetic Resonance in Medicine, 2018. **00**: p. 1-17.
149. Jeurissen, B., et al., *Diffusion MRI fiber tractography of the brain.* NMR in Biomedicine, 2019. **32**(4): p. e3785.
150. Vercelli, A., et al., *Recent techniques for tracing pathways in the central nervous system of developing and adult mammals.* Brain research bulletin, 2000. **51**(1): p. 11-28.
151. Hubbard, P.L., et al., *Biomimetic phantom for the validation of diffusion magnetic resonance imaging.* Magnetic resonance in medicine, 2015. **73 1**: p. 299-305.
152. Takemura, H., et al., *A major human white matter pathway between dorsal and ventral visual cortex.* Cerebral cortex, 2016. **26**(5): p. 2205-2214.
153. Zalesky, A., *DT-MRI fiber tracking: a shortest paths approach.* IEEE transactions on medical imaging, 2008. **27**(10): p. 1458-1471.
154. de Reus, M.A. and M.P. Van den Heuvel, *The parcellation-based connectome: limitations and extensions.* Neuroimage, 2013. **80**: p. 397-404.
155. Schilling, K., et al., *Can increased spatial resolution solve the crossing fiber problem for diffusion MRI?* NMR in Biomedicine, 2017. **30**(12): p. e3787.
156. Zhan, L., et al., *Magnetic resonance field strength effects on diffusion measures and brain connectivity networks.* Brain connectivity, 2013. **3**(1): p. 72-86.
157. Ambrosen, K.S., et al., *Validation of structural brain connectivity networks: The impact of scanning parameters.* NeuroImage, 2020. **204**: p. 116207.
158. Schilling, K.G., et al., *Brain connections derived from diffusion MRI tractography can be highly anatomically accurate—if we know where white matter pathways start, where they end, and where they do not go.* Brain Structure and Function, 2020. **225**(8): p. 2387-2402.
159. Chu, S.-H., K.K. Parhi, and C. Lenglet, *Function-specific and enhanced brain structural connectivity mapping via joint modeling of diffusion and functional MRI.* Scientific reports, 2018. **8**(1): p. 1-19.
160. Zalesky, A., et al., *Connectome sensitivity or specificity: which is more important?* Neuroimage, 2016. **142**: p. 407-420.

161. Gatto, R.G., et al., *Ultra-high field diffusion MRI reveals early axonal pathology in spinal cord of ALS mice.* Translational neurodegeneration, 2018. **7**(1): p. 1-14.
162. Alexander, D.C., G.J. Barker, and S.R. Arridge, *Detection and modeling of non-Gaussian apparent diffusion coefficient profiles in human brain data.* Magnetic resonance in medicine, 2002. **48 2**: p. 331-40.
163. Anderson, A.W., *Measurement of fiber orientation distributions using high angular resolution diffusion imaging.* Magnetic resonance in medicine, 2005. **54 5**: p. 1194-206.
164. Jansons, K.M. and D.C. Alexander, *Persistent angular structure: new insights from diffusion magnetic resonance imaging data.* Inverse problems, 2003. **19**(5): p. 1031.
165. Nath, V., et al., *Empirical estimation of intravoxel structure with persistent angular structure and Q-ball models of diffusion weighted MRI.* Journal of Medical Imaging, 2018. **5**(1): p. 014005.
166. Sweet, A. and D. Alexander. *Reduced encoding persistent angular structure*. in *International society for magnetic resonance in medicine*. 2010.
167. Yeh, F.-C., V.J. Wedeen, and W.-Y.I. Tseng, *Generalized q-Sampling Imaging.* IEEE transactions on medical imaging, 2010. **29**(9): p. 1626-1635.
168. Henderson, F., et al., *Tractography and the connectome in neurosurgical treatment of gliomas: the premise, the progress, and the potential.* Neurosurgical focus, 2020. **48**(2): p. E6.
169. Tran, G. and Y. Shi, *Fiber orientation and compartment parameter estimation from multi-shell diffusion imaging.* IEEE transactions on medical imaging, 2015. **34**(11): p. 2320-2332.
170. Yang, S., et al., *A Simplified Crossing Fiber Model in Diffusion Weighted Imaging.* Frontiers in neuroscience, 2019. **13**: p. 492.
171. Basser, P.J. and S. Pajevic, *Statistical artifacts in diffusion tensor MRI (DT-MRI) caused by background noise.* Magnetic resonance in medicine, 2000. **44 1**: p. 41-50.
172. Weinstein, D., G. Kindlmann, and E. Lundberg. *Tensorlines: Advection-diffusion based propagation through diffusion tensor fields*. in *Proceedings of the conference on Visualization'99: celebrating ten years*. 1999. IEEE Computer Society Press.
173. Lazar, M., et al., *White matter tractography using diffusion tensor deflection.* Human brain mapping, 2003. **18**(4): p. 306-321.
174. Jiang, H., et al., *DtiStudio: resource program for diffusion tensor computation and fiber bundle tracking.* Computer methods and programs in biomedicine, 2006. **81**(2): p. 106-116.
175. Parker, G.J. and D.C. Alexander. *Probabilistic Monte Carlo based mapping of cerebral connections utilising whole-brain crossing fibre information*. in *Biennial International Conference on Information Processing in Medical Imaging*. 2003. Springer.
176. Parker, G.J. and D.C. Alexander, *Probabilistic anatomical connectivity derived from the microscopic persistent angular structure of cerebral tissue.* Philosophical transactions of the Royal Society B: Biological sciences, 2005. **360**(1457): p. 893-902.
177. Behrens, T.E.J., et al., *Characterization and propagation of uncertainty in diffusion-weighted MR imaging.* Magnetic resonance in medicine, 2003. **50 5**: p. 1077-88.
178. Christiaens, D., et al., *Global tractography of multi-shell diffusion-weighted imaging data using a multi-tissue model.* Neuroimage, 2015. **123**: p. 89-101.
179. Neher, P.F., et al. *MITK global tractography*. in *Medical Imaging 2012: Image Processing*. 2012. International Society for Optics and Photonics.